

The Nitrogen-to-Oxygen evolution in galaxies: the role of the star formation rate

M. Mollá,¹★ J. M. Vílchez,² M. Gavilán,³ and A. I. Díaz³

¹Departamento de Investigación Básica, C.I.E.M.A.T. Avda. Complutense 22, 28040, Madrid, (Spain)

²Instituto de Astrofísica de Andalucía (CSIC), Apdo. 3004, 18080 Granada, Spain

³Departamento de Física Teórica, Universidad Autónoma de Madrid, 28049 Cantoblanco, Madrid (Spain)

Accepted Received ; in original form

ABSTRACT

The main objective of the present work is to check if the star formation efficiency plays a relevant role in the evolution of the relative abundance N/O. In order to explore this idea, we analyze the evolution of the nitrogen-to-oxygen ratio as predicted by a set of computed theoretical models. These models consist of simulated galaxies with different total masses which are evolved assuming different collapse time scales and different star formation efficiencies. The combinations of these two parameters produce different star formation histories, which in turn have, as we show, an important impact on the resulting N/O ratio. Since we want to check the effect of variations in these efficiencies on our models results, the same stellar yield sets are used for all of them. The selected yields have an important contribution of primary nitrogen proceeding from low and intermediate mass stars, which implies that N is ejected with a certain delay with respect to O. It allows to obtain, as we demonstrate, a dispersion of results in the N/O-O/H plane when star formation efficiencies vary which is in general agreement with observations. The model results for the N/O abundance ratio are in good agreement with most observational data trends. In particular, the behavior shown by the extragalactic H_{II} regions is well reproduced with present time resulting abundances. Furthermore, the low N/O values estimated for high-redshift objects, such as those obtained for Damped Lyman Alpha (DLA) galaxies, as well as the higher (and constant) values of N/O observed for irregular and dwarf galaxies or halo stars, can be simultaneously obtained with our models at the same low oxygen abundances $12 + \log(O/H) \sim 7$. We therefore conclude that, even though there seems to be a general believe that abundance ratios depend mostly on stellar yields, these are not the only parameter at work when both elements are ejected by stars of different mass range, and that differences in the star formation history of galaxies and regions within them are a key factor to explain the data in the N/O-O/H plane.

Key words: galaxies: abundances – galaxies: evolution – galaxies: spirals – galaxies: dwarf – galaxies: irregular – galaxies: stellar content

1 INTRODUCTION

The nitrogen abundances have posed an important debate which lasts up to now. First, because it is created in two types of stars, what rises the doubt about which proportion is produced in massive stars and how much N is ejected by low and intermediate mass (LIM) stars. Second, the possible primary or secondary origin of nitrogen implies some questions about what is the contribution of each type produced in each star. The question is then how much N is created in each stellar mass range and what fraction of it is primary?

From an observational point of view, the need for a primary component of N appeared very soon. Edmunds & Pagel (1978)

and Alloin et al. (1979) already concluded, from the analysis of the then available extragalactic H_{II} region data, that N behaves, at least partially, as a primary element. This was later supported by N measurements for Galactic metal-poor halo stars (Barbuy, 1983; Tomkin & Lambert, 1984; Laird, 1985; Carbon et al., 1987), and by additional extragalactic H_{II} region observations (McCall et al., 1985; Vila Costas & Edmunds, 1993). The number of N data points has increased extraordinarily since then (see Henry et al., 2000; Contini et al., 2002, and references therein) showing the same basic trend: 1) a strong slope for the N/O data against oxygen abundance for metal-rich regions, a well explained behaviour by the secondary character expected from the CNO cycle production, and 2) a flat line for the data of low mass and irregular galaxies and halo stars with $12 + \log(O/H) < 8$. Some very recent observations of halo stars (Israelian et al., 2004; Spite et al., 2005) have increased the

★ E-mail:mercedes.molla@ciemat.es

number of data in the low abundance end. They show a large scatter in N/O at low metallicities, and some high N/O ratios, implying an important primary N production at very early evolutionary times.

Since low metallicity galaxies have been considered to be young objects undergoing their first burst of star formation (Thuan et al., 1995), it was assumed that they have had no time for their LIM stars to evolve and eject the nitrogen produced by them. Moreover, the dispersion found for their N/O abundances was really low. This way, a number of authors have claimed that massive stars are the main primary N producers. There are two facts against this argument: 1) these galaxies are not so young as it was thought, since recent observations indicate that they host stellar populations which are at least $10^7 - 10^8$ yr old, reaching even 1 Gyr in some cases (Legrand, 2000; Tolstoy, 2003; Cairós et al., 2003; van Zee et al., 2004; Thuan & Izotov, 2005); 2) if LIM stars with masses in the range $4-8 M_{\odot}$ eject some amount of primary N, this can be in the interstellar medium (ISM) within a time as short as $\sim [50 - 200]$ Myr, since the mean-lifetimes of these stars are in this range. Moreover, low oxygen abundance do not necessarily imply short time-scales. In fact, we claim that it is essential to change the usual scheme that identify oxygen abundances with evolutionary time, a misunderstander concept that lead to erroneous conclusions.

On the other hand, there is no clear mechanism which may produce primary N in massive stars. Some authors working on stellar evolution have searched for new possibilities, the most plausible one being the effect of rotation on stars. Meynet & Maeder (2002) have computed some yields from stellar models including rotation obtaining that intermediate and massive stars may produce primary N, mostly at very low metallicity. However, Chiappini et al. (2005) have included these yields in a Galactic chemical evolution (GCE) model finding that an extra-production of N in low metallicity massive stars by a large factor, between 40 and 200 along the mass range, is still necessary to explain the data for very metal-poor halo stars since the yields used do not produce a sufficient amount of primary N. Recently, Chiappini et al. (2006) use new (and still unpublished) yields for metal-poor massive stars which rotate rapidly thus producing large amounts of primary nitrogen with which it is possible to increase the N/O abundance up to similar levels of the Galactic halo stars. These preliminary yields are still uncertain since they are computed assuming a non-observed very high rotation velocity for these low-metallicity stars.¹.

The situation has become more complicated because abundances of N for DLA galaxies have been derived (Pettini et al., 2002; Prochaska et al., 2002; Centurión et al., 2003, and references therein). When these recent observations are included in the sample, a large dispersion appears, in evident disagreement with the hypothesis of all the primary N being produced by massive stars. DLA data show lower values of N/O than those, populating the flat slope, obtained for the irregular and blue compact galaxies and for the halo stars of similar oxygen abundance. These high redshift objects have oxygen abundances which correspond to slightly evolved objects as those observed in the local universe, but in this case some values of N/O are much smaller than the local ones. This fact appears incompatible with primary N being produced by massive stars, as those very metal-poor ones rotating at very high velocity used in Chiappini et al. (2006), since in that case it results

difficult to conceive which mechanism could produce a different final yield (and therefore a different point on the N/O-O/H plane) for each DLA object.

From the theoretical point of view, a secondary production is expected in most stars, as corresponds to the CNO cycle, while the primary contribution should arise from intermediate mass stars ($4 \leq M/M_{\odot} \leq 8$). These stars may suffer, during the Asymptotic Giant Branch (AGB) phase, dredge-up episodes and hot bottom burning processes, due to which some primary N may be created. This fact has been well known for some decades (Renzini & Voli, 1981; Serrano, 1986). In fact, most of yield sets (as van den Hoek & Groenewegen, 1997; Marigo et al., 1998) presently used for the chemical evolution models include a contribution of primary N produced by these processes in LIM stars. The AGB phase is still far from being well understood, and there exist large uncertainties about the exact amount of primary nitrogen produced through the HBB process. Probably due to that reason, the up to now computed models do not seem be able to reproduce most of the data.

The idea that a constant N/O may only be obtained with a primary N from massive stars is indeed an oversimplification which does not take into account the stellar lifetimes. Vila Costas & Edmunds (1993) and Pilyugin et al. (2003), by analyzing the N/O values in galaxies of different morphological type, concluded that a long-time-delayed contribution to the N production must exist. Vila Costas & Edmunds (1993) suggested that most data fall in a region limited by two extreme closed box models defined by distinct delays, produced by different star formation efficiencies, and/or ages of galaxies, thus explaining the observed dispersion.

This way, Henry et al. (2000) and Prantzos (2003) – hereinafter HEN and PRAN, respectively – computed realistic chemical evolution models using yields from van den Hoek & Groenewegen (1997) for LIM stars, with a contribution of primary N. Although their models produce a level of N/O higher than observations for Z low, they show that, actually, a N/O vs O/H relation much flatter than usual may be obtained with their models, only decreasing the efficiencies of star formation. The same finding was also obtained by Larsen et al. (2001) using several sets of yields, all of them with a proportion of primary N ejected by LIM stars. These results lead to the idea that stellar yields are not the only driver of the N/O ratio, at least when LIM stars produce a quantity of primary N, and that most observations in the plot N/O-O/H might be reproduced if different star formation rates in the different galaxies or regions are considered

Gavilán et al. (2005) and Gavilán et al. (2006, hereinafter GAV05 and GAV06, respectively) have recently calculated some chemical evolution models for the Milky Way Galaxy (MWG), by using different sets of stellar yields. They demonstrated in those works that a model using the set of yields for LIM stars from Gavilán et al. (2005) joined to the massive stellar yields from Woosley & Weaver (1995) is able to reproduce most of trends of MWG data. In the cited model, a flat behaviour of N/O vs O/H appears when the star formation rate is low during a long time, as it occurs in the Galactic halo or in the the outer regions of the Galactic disc. In this case, since the evolution is slow, a time longer than 40 Myr is necessary to reach oxygen abundances $12 + \log(O/H) \sim 7$, which is sufficient for LIM stars to eject their products to the ISM. This, combined with low O/H abundances, produces high N/O values, similar to those observed, for low abundances. Most of the data of the Galaxy halo and disc, in particular those of nitrogen – see their Fig.12 –, are successfully reproduced with that model.

¹ In fact, as Hirschi (2005) stated, the ratio v_{ini}/v_c decreases at very low metallicity for the initial velocity of 300 km s^{-1} because stars are more compact at lower metallicity.

Furthermore, the model results for the radial regions other than the Solar Neighbourhood suggest that actually the dispersion observed in MWG data can be a consequence of different star formation histories (produced by different collapse timescales to form the disc and different efficiencies to form stars) in the Galactic radial regions. This supports the mentioned findings from the above cited authors: different evolutionary tracks and end points in the O/H-N/O plane are possible simply by increasing or decreasing the star formation rate, although other parameters probably also play a role.

The objective of this work is, therefore, to explore if different star formation efficiencies may produce different tracks in the N/O-O/H plane and to check, with a wide grid of chemical evolution models, if the results are acceptable as compared with the observational data trends. In order to do this task we need a large number of models with the same basic assumptions about the evolution and where only the star formation be varied. Therefore, we analyze the results obtained for the evolution of nitrogen with the wide grid of models shown in Mollá & Díaz (2005), which simulates 44 galaxies with different total masses and 10 possible star formation efficiencies. The chosen sets of yields used for these computations were those from WW for massive stars and those from GAV05 for LIM stars, which were already calibrated as explained above. An advantage of using these yields is that the primary N proceeds from LIM stars with which the effect of variable star formation is probably more evident.²

In Sect. 2 we analyze the N/O-O/H results obtained with simple chemical evolution models, by describing how elemental abundances of N and O evolve. In Sect. 3 we summarize the resulting abundances for the multiphase chemical evolution model with a contribution of primary nitrogen proceeding from LIM stars variable with Z. Sect. 4 is devoted to the results obtained when the same code is applied to a wide grid of simulated galaxies with different masses and star formation efficiencies. Our conclusions are in Sect. 5.

2 THE CLOSED BOX MODEL PREDICTIONS

Nitrogen needs a seed of carbon or oxygen to be created from the CNO cycle. If this seed already exists when the star forms, N will be produced as a secondary element, what implies that its relative abundance N/C (or N/O) will increase proportionally to the original abundance of C or O. If the seed is created in the same star, just before N, then N is primary, and its abundance will be proportional to the C or O abundance, that means that N/C or N/O will maintain a constant value. Both trends are easily obtained using the classical and well known *closed box model* (hereinafter CBM) following which the abundance of an element i , Z_i , is related on the gas fraction, $\mu = g/M$, or ratio of the gas mass to the total mass in the region (Pagel et al., 1979; Tinsley, 1980), through the expression: $Z_i = p_i \ln \mu^{-1}$, where p_i is the stellar yield, the new production of an element i by a generation of stars. If nitrogen and oxygen would be both primary, with yields $p_N = ppN$ and $p_O = pO$, respectively, then the relative abundance Z_N/Z_O is:

² Since the objective of this work is to explore if different star formation efficiencies produce different tracks in the N/O-O/H plane we must use the same ingredients for all our realizations, except the parameter we want to check. This is similar to the usually applied method when the stellar yields are the free parameters. In that case using the same ingredients, except the stellar yields, for some Galactic chemical evolution (GCE) models, it is possible to determine what set of yields is the most adequate.

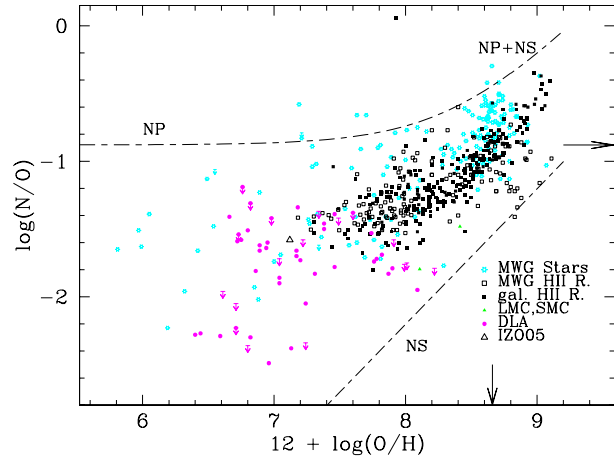


Figure 1. The relative abundance $\log(N/O)$ as a function of the oxygen abundance, $12 + \log(O/H)$, when N is secondary, shown by the line NS, primary, marked as NP, or a combination of both primary + secondary, marked as NP+NS. The points are the available data taken from references of Table 1 for stars of our Galaxy, Galactic and external galaxy HII regions, LMC and SMC galaxies and DLA objects as labelled. The data for the lowest metallicity known galaxy (SBS0335-052) from Izotov et al. (2005) is marked as an open triangle. The arrows mark the solar values in the graph and the short-long-dashed lines limit the region occupied by the observational data.

$$\frac{Z_N}{Z_O} = \frac{ppN}{pO} = cte \quad (1)$$

It, instead, nitrogen is secondary, its stellar yield $p_N = psN$ will depend on the abundance of the seed, in this case Oxygen. Then: $p_N = psN \times Z_O$, and therefore:

$$\frac{Z_N}{Z_O} = \frac{psN}{2pO} Z_O \quad (2)$$

Actually, the mechanism to form N in stars is mostly secondary, with a behaviour as the one shown by the line named NS in Fig. 1. However, the observed data (taken from references given in Table 1), indicate, such as we may see in the same figure, that a primary contribution of N is necessary to explain the behaviour of data in the Universe. A line as this one marked with NP shows the expected behaviour with a primary contribution plus a secondary one. This last one is only apparent when the oxygen abundance is high enough ($12 + \log(O/H) > 7.5 - 8$), marked as NP+NS. Obviously, if we change the yield ppN or psN , the lines would move toward higher or lower N/O abundances. The two lines shown in the figure have, in fact, been drawn to show the possible range of the data. It is clear that only a line cannot explain the observed dispersion but is also evident that both components are necessary to obtain the trend shown by the data.

Nevertheless, a primary behaviour does not imply necessarily a constant value of N/O for the whole time evolution since we must take into account the mean-lifetimes of stars. The above results are obtained, as usual, with the classical hypotheses in the closed box model that all stellar products are ejected simultaneously in the ISM. Some primary nitrogen is easily produced by LIM stars in the range of $[4-8] M_\odot$ (Renzini & Voli, 1981; van den Hoek & Groenewegen, 1997; Marigo et al., 1998; Gavilán et al., 2005) during the Hot Bottom Burning (HBB) process. Since these stars died after the bulk of oxygen created by massive stars was ejected, if they are the main producers of primary N, this N would appear in the ISM later than the oxygen does. In

Table 1. References for N and O stellar abundances used for the comparison

MWG Stars
Clegg et al. (1981)
Daflon & Cunha (2004)
Gratton et al. (2000)
Gummersbach et al. (1998)
Israelian et al. (2004)(ISR)
Smartt et al. (2001)
Spite et al. (2005)(SPI)
MWG HII Regions
Carigi et al. (2005)
Esteban et al. (1999,?,?)
Fich & Silkey (1991)
Peimbert (1979)
Shaver et al. (1983)
Tsamis et al. (2003)
Vilchez & Esteban (1996)
External Galaxies HII Regions
Garnett et al. (1995, 1999)
Izotov & Thuan (1999)
Izotov et al. (2005)
Nava et al. (2005)
Tsamis et al. (2003)
van Zee et al. (1998, 2006)
van Zee & Haynes (2006)
Damped Lyman Alpha Objects
Centurión et al. (2003)
Prochaska et al. (2002)
Pettini et al. (2002)

this scheme, if the necessary NP was ejected by the LIM stars, one would expect that N/O will be flat only after the oxygen has already reached a certain level of abundance, giving time to nitrogen to appear, but it will not be constant before that moment.

In that case the evolution of the N abundance is given by the following equation, taken from Henry et al. (2000,Ap.B):

$$Z_N = \frac{ppN}{pO} \exp\left(\frac{Z_\tau}{pO}\right) (Z - Z_\tau) * F + \frac{psNppC}{2pO^2} Z^2 + \frac{psNpsC}{6pO^2} Z^3, \quad (3)$$

where ppC and psC refer to the carbon primary and secondary yields, analog to ppN and psN , and F is a step function that has a value of zero except if $Z > Z_\tau$. The abundance of N is, this way, computed as a function of the oxygen abundance, $Z = Z_0$, which will be ejected by short mean-lifetimes massive stars, that is almost immediately after the formation of the first stars. The nitrogen has a secondary component that also appears in the ISM from early times (second and third terms), and other primary contribution, only produced by LIM stars, which will appear in the ISM with a certain delay (first term).

This delay translates in that the primary N will appear only when the oxygen abundance has already reached a certain value Z_τ , reached in the time when the LIM stars died. Actually, the LIM stars have not large mean-lifetimes τ . Using the age-stellar mass relation obtained by the Geneva group isochrones (Schaller et al.,

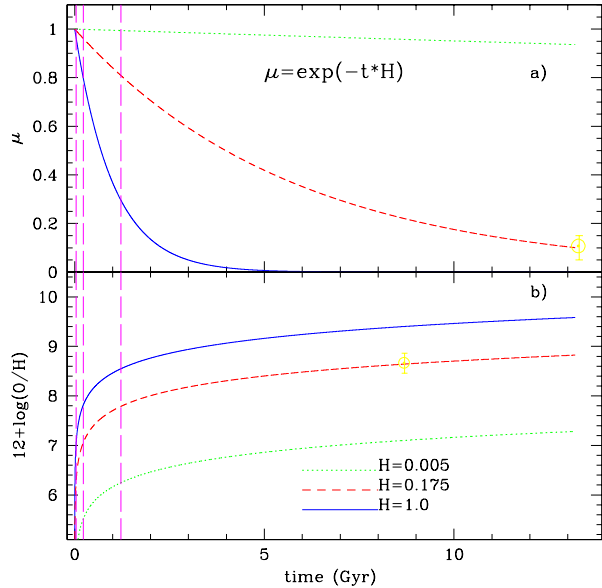


Figure 2. a) The time evolution of the fraction of gas $\mu = \exp(-tH)$ for three different values of $H = 0.005, 0.175$, and 1 as given in the bottom panel; b) The time evolution of the oxygen abundance $12 + \log(O/H)$ for the same models than a). The long-dashed (magenta) lines mark the times $t = 0.040, 0.221$ and 1.21 Gyr. The Solar region values are indicated in both panels.

Table 2. Values of oxygen abundances Z_τ reached when LIM stars die for different values of the parameter H .

M_{star} M_\odot	H_1	H_2	H_3
2	0.399e-2	0.695e-3	0.200e-4
4	0.729e-3	0.131e-3	0.376e-5
8	0.123e-3	0.229e-4	0.660e-6

1992), stars of $2, 4$, and $8 M_\odot$, have mean-lifetimes of $\tau \sim 1.21, 0.228$, and 0.040 Gyr, respectively, short in chemical evolution terms. In order to calculate the abundances Z_τ reached when these stars die, we use again the CBM: $Z_\tau = p \ln \mu^{-1}(t = \tau)$. For computing the values of the gas fraction, at those times, we assume that it is a decreasing exponential function of time: $\mu(t) = \exp(-tH)$, where H is the efficiency to form stars (equal to the inverse of the time-scale for consuming the gas, $1/\tau_{gc}$). We show in Fig. 2a the time evolution of this function $\mu(t)$ for 3 different values of $H = 0.005, 0.175$, and 1.0 (or $\tau_{gc} = 200, 5.75$, and 1 Gyr). In panel b) we show the time evolution of the oxygen abundance, as $12 + \log(O/H)$, corresponding to each one of these parameters H . We give in Table 2 the values of Z_τ reached in these closed models when $t = \tau$ for stars of $2, 4$, and $8 M_\odot$ computed using $pO = 3.3E - 3$, $ppC = 1.2E - 3$, $psC = 0.9$, $ppN = 2.2E - 4$ and $psN = 0.130$. as stellar yields for Oxygen, primary and secondary Carbon, and primary and secondary Nitrogen, respectively.

In Fig. 3a) we show how the N/O evolves when O/H increases in the model corresponding to $H = 0.175$ for the three possible values of column 3 of Table 2, which would be the oxygen abundance

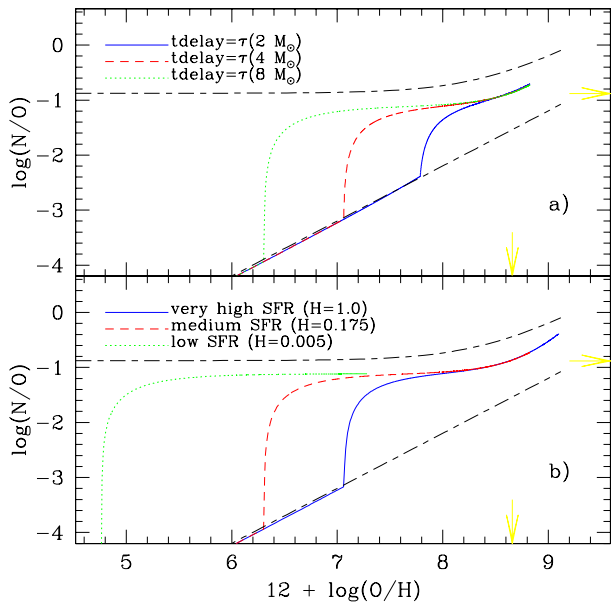


Figure 3. The relation of $\log(N/O)$ with the oxygen abundance $12 + \log(O/H)$, by assuming that the gas fraction is an exponential decreasing function of time, obtained by Eq.(4) with two contributions. The primary component appears in the ISM: a) when stars of 2, 4 and $8 M_{\odot}$ die, dotted (green), short-dashed (red) and solid (blue) lines, respectively, with a parameter $H = 0.175$; b) when stars of $8 M_{\odot}$ die by assuming different values for H as marked in the figure. The short-long-dashed lines and the (yellow) arrows have the same meaning than in Fig. 1.

reached by assuming a primary N proceeding from stars of 2, 4 and $8 M_{\odot}$. We may distinguish three phases in that figure:

(i) The N/O increases smoothly as secondary from the first phases of the evolution, for $Z < Z_{\tau}$, with a clear slope that corresponds to the secondary contribution of massive stars.

(ii) The NP appears in the ISM when $Z = Z_{\tau}$, increasing very rapidly the relative abundance (N/O). The final value of this phase is given by $\frac{ppN}{pO}$. This feature must not be erroneously taken as a secondary behaviour.

(iii) After this exponential function, the secondary behaviour proceeding from LIM stars³ appears again.

Two evident facts appear in that graph:

- The change from the NS to the NP regime occurs very abruptly.

- The oxygen abundance at which this change occurs is very dependent on the star formation rate and on the mass of the first stars ejecting primary nitrogen.

Obviously, if NP would be ejected by stars of $2 M_{\odot}$, which is not a realistic case, there would be more time for oxygen abundances to increase, and so the value Z_{τ} would be higher than in the case of NP ejected by stars of $8 M_{\odot}$. In the last case ($8 M_{\odot}$), the abrupt increase of N/O appears at the left in the figure N/O – O/H, while the first one ($2 M_{\odot}$) produces this increase at the right of the figure. The higher the mass of the stars ejecting NP, the lower the oxygen abundance for which the change takes place.

³ We have used the same psN for both massive and LIM stars although it may have a different value for each mass range.

On the other hand, it is also evident that these Z_{τ} abundances, shown in Table 2, depend on the star formation rate: in Fig. 3b) we show the results obtained using the values Z_{τ} shown in the last line of Table 2, assuming that stars of $8 M_{\odot}$ are the responsible in producing NP. If the star formation rate is strong ($H = 1.0$, solid line) the oxygen abundance increases very rapidly, so when the primary nitrogen begins to be ejected, O/H has already reached a high value. On the contrary, if the star formation rate is low ($H = 0.005$, dotted line), Oxygen maintains a low abundance for a long time. It is, therefore, possible that Nitrogen to be ejected when O/H is still below $12 + \log(O/H) < 7$.

The closed box model provides approximated results, even for oxygen abundances, since it is valid only if $Z \ll 1$ which is not longer valid when the fraction of gas is small. Furthermore, the hypothesis of a gas fraction decreasing with time is not valid for a disc which forms from the gas in-falling from the halo. In fact, the evolution of the gas fraction predicted by a CBM with $H = 0.175$, which might represent the Solar vicinity, is very similar to the one obtained with a numerical model by GAV05 for the Solar region. Both models differ, however, at the earliest phases: first, the numerical model maintains a higher value than the equivalent CBM, and then it rests below this last one. Finally, both reach a similar value of ~ 0.10 as observed. The oxygen abundances are not equivalent, too, to the CBM ones. The GAV05 model lasts more time to reach to an oxygen abundance $12 + \log(O/H) = 7$. This occurs just when the first LIM stars begin to die, so it is important to remind that, in a realistic case, when LIM stars begin to die, the oxygen abundance may be even lower than predicted by a CBM model.

In summary, the stellar yields and the mass range of stars (or their mean-lifetimes) that produce nitrogen are important to determine the possible evolution of N/O vs O/H but the star formation history results also essential to determine what is the track followed by a given region or galaxy in the plane N/O-O/H.

3 THE MULTIPHASE CHEMICAL EVOLUTION MODEL

3.1 Abundance calculations

Now we use a numerical code which takes into account the stellar mean-lifetimes and other more realistic assumptions for the scenario and input prescriptions (infall rate, masses, geometry, etc). The next calculations have been performed with the multiphase model, a numerical code developed by Ferrini et al. (1992), and widely described in that work and in the following ones (Ferrini et al., 1994; Mollá et al., 1996) of the same group.

As it is explained in Ferrini et al. (1992), the equation to compute the abundances of each element i in the gas, X_i , is:

$$\frac{dX_i g_D}{dt} = -X_i \Psi + X_{i,H} f g_H + W_i(t) \quad (4)$$

W_i being the ejected mass rate (new + old) for each element i by the stars, g_D the gas mass, Ψ the star formation rate in the modeled disc region and $f g_H$ the infall rate, assuming as usual that there exists a gas infall from the halo to the disc. The ejected metals mass rates or restitution rates $W_i(t)$ are computed following the formalism of the Q's matrices, well described in the cited work (Ferrini et al., 1992) and also in other works, as Portinari et al. (1998). We recommend these works to the reader for a clear explanations of equations.

The expression to compute the term W_i is:

$$W_i(t) = \int_{m,\tau=t}^{mup} \sum_j \tilde{Q}_{i,j}(m) X_j(t - \tau(m)) \Psi(t - \tau(m)) dm \quad (5)$$

where the expression $\tilde{Q}_{i,j} = Q_{i,j}\Phi(m)\Phi(m)$ represent the matrix $Q_{i,j}$ multiplied by the initial mass function $\Phi(m)$, and $Q_{i,j}$ are defined as:

$$Q_{i,j}(m) = \frac{mexp_{i,j}}{m_j} = \frac{mexp_{i,j}}{mX_j} \quad (6)$$

$mexp_{i,j}$ being the ejected mass of each element i which was originally in the star as element j . This way, the total fraction of element i ejected by each type of stars with mass m is:

$$\frac{mexp_i(m)}{m} \Phi(m) = \sum_j \frac{mexp_{i,j}}{m} \Phi(m) = \sum_j \tilde{Q}_{i,j}(m) X_j \quad (7)$$

When there are two components primary and secondary for an element, as it occurs with N, it is necessary to know both contributions for each star and to compute them separately in the model. The multiphase model uses for that the equations shown in Ferrini et al. (1992), similar to those shown by Portinari et al. (1998) in their Appendix B.

3.2 Parametric study

The above cited expressions are those included in the multiphase chemical evolution code from Ferrini et al. (1992, 1994) where yields from Renzini & Voli (1981, RV) for LIM stars and from Woosley & Weaver (1986, WW86) for massive stars were used to model the Galactic chemical evolution. Taking into account our previous findings, it is evident that not only the stellar yields play a role in the resulting evolution of N in a region or galaxy. The star formation history is very important in determining the track followed by a given object in the plane N/O-O/H. A distinct feature is shown in this plane when the primary nitrogen is ejected to the ISM; and this feature appears at higher or lower oxygen abundances depending on the star formation rate: the stronger the star formation rate, the highest the oxygen abundance at which this characteristic increase appears. Therefore, it is necessary to analyze how N evolves when different input parameters, related to the star formation rate, are chosen for a given multiphase chemical evolution model as this one used in Ferrini et al. (1994).

We, therefore, analyze in detail this influence of these input parameters (see Mollá & Díaz, 2005, for a wide explanation of the multiphase model and its parameters) over the N/O evolution. For that, we have computed some family of generic models, (that is, they are not models applicable to MWG) all of them using only a matrix Q corresponding to one metallicity:

- (i) Three models where the star formation rate in the halo, represented by its efficiency ϵ_K , takes three different values: $\epsilon_K=0$, $\epsilon_{K,std}$, and $100 \times \epsilon_{K,std}$, where $\epsilon_{K,std}$ is the value used in Ferrini et al. (1994), and subsequent multiphase models, for the MWG halo.
- (ii) Three models where there is no star formation in the halo, $\epsilon_K = 0$, and where only the density of the initial mass gas change from a model to the following one.
- (iii) Three models where there is no star formation in the halo, $\epsilon_K = 0$, and where efficiencies to form stars are the same, but with a total mass and an infall rate different for each model.
- (iv) Three models where there is no star formation in the halo, $\epsilon_K = 0$, and where the total mass and the infall rate is the same for all models, but where efficiencies to form stars are different for each one.

The results of these models are shown Fig. 4. In each panel we show the variations on the N/O track by the change of one parameter as described. Its is clear from these results that there are some parameters who may change the N evolution since the early phases of the evolution. Only in panel b) N/O shows a similar evolution for all densities. Instead, the evolution of N/O depends very strongly on the star formation rate (either in the halo or in the disc). The effect of the halo star formation is only evident if ϵ_K is so high. If it is low enough the variations for $12 + \log(O/H) > 6$ are indistinguishable in the resulting track.

As before, the N/O evolution shows a flatter or a steeper behaviour depending on the type of scenario or model defined by the parameters of star formation in the halo, the possible infall rate from the halo to the disc, and the star formation rate in the disc. We recall that a strong star formation in the halo in the earliest phases of the evolution, before stars form in the disc, as it is thought it occurred in our Galaxy, produces a shift of the N/O track in the plane N/O-O/H toward high oxygen values and an steep similar to this shown in Fig. 3 for the model in which the primary nitrogen is ejected by the lowest mass stars. On the other hand, if there is no star formation in the halo, as occurs in the three other panels, or it is low enough, the abrupt *change of phase* disappears in our graphs, just because it occurs at lower oxygen abundances than those shown of the figure. This way the track simulates a smoother behaviour. Therefore, variations of input parameters and scenarios may explain, at least partially, the differences found when chemical evolution models in the literature, using the same set of yields, are compared.

The old version of the Galactic multiphase chemical evolution model from Ferrini et al. (1992, 1994) was computed with the same efficiency to form stars and molecular clouds for all MWG disc regions, but using collapse timescales variable with the galactocentric radius of each radial region, different total masses, and taking into account the differences in the geometry, that is the effect of the volume over the densities. And, hence, the resulting star formation histories show higher and earlier maximum values at the inner regions of the disc than at the outer ones. Thus, the results for different radial regions of the disc already shown a behaviour in agreement with the previous section: a more *secondary* track for the strong star formation regions of the inner disc, and less steeper for the outer regions ones in which the star formation resulted smoother.

3.3 The effect of the metallicity dependent yields

The stellar models and their corresponding yields of elements depend now on metallicity, and, therefore, a set of matrices Q's for each metallicity is used⁴.

We have computed a Galactic chemical evolution model following the same prescriptions given in Ferrini et al. (1994) and

⁴ Such as Ferrini et al. (1992); Portinari et al. (1998) claim the $Q_{i,j}$ formalism have some advantages since it compensates the lack of metallicity dependent yields. One may think that the use of matrices Q's may be avoided when this kind of yields are already available. However, such as Portinari et al. (1998) explained: ... *stellar models with different metallicities generally assume solar relative abundances of the various species within a given Z; but abundance ratios are not constant in the course of galactic evolution, nor they are in the evolution of a chemical model. The matrix links any ejected species to all its different nucleosynthetic sources, allowing the model to scale the ejecta with respect to the detailed initial composition of the star through the Q's.* Therefore, as these authors we continue using the same formalism.

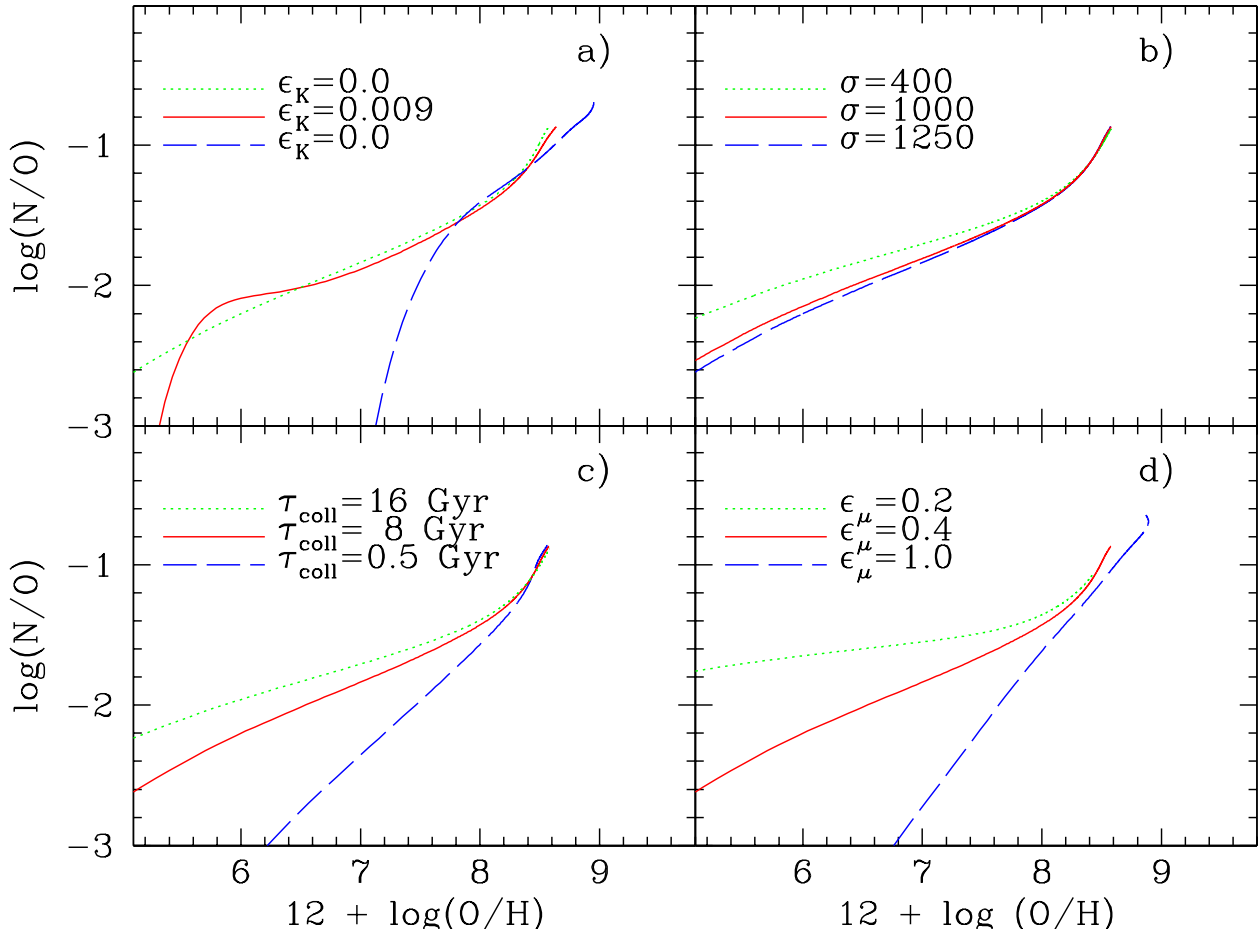


Figure 4. The effect of varying the input parameters of some generic chemical evolution models on the evolution of the relative abundance $\log(\text{N}/\text{O})$ vs the oxygen abundance $12 + \log(\text{O}/\text{H})$: a) The effect of the star formation of the halo; b) The effect of the different initial density of gas mass in the region; c) the effect of the infall gas rate; d) the effect of the star formation efficiencies.

Portinari et al. (1998) but using the metallicity dependent yields from van den Hoek & Groenewegen (1997) for LIM stars and WW95 for massive stars. The resulting model reproduces well the star formation history and the age-metallicity relation for the Solar vicinity, as it is shown in GAV05. The radial distributions of diffuse and molecular gas, star formation rate and oxygen abundance also fit the observational constraints.

In Fig. 5 we represent the evolution of $\log(\text{N}/\text{O})$ vs $12 + \log(\text{O}/\text{H})$ for this model. In each panel we compare the results for an outer, medium and inner Galactic disc region, as labelled in the figure, (solid line), with CBM models (dotted lines) computed assuming that NP appears when stars of $6 M_{\odot}$ die. The values for the abundance Z_{τ} , shown in Table 3, are taken from the same multiphase models for $t = \tau(6M_{\odot})$.⁵ In this case we have used the set with $\eta_{AGB} = 4$ and $m_{HBB} = 0.8M_{\odot}$ of metallicity dependent yields from van den Hoek & Groenewegen (1997), which have been in-

cluded in the CBM, after a fit with least squares functions, by the expressions:

$$ppN = 1.0E - 8 \times z_{\tau}^{-0.76} \quad (8)$$

and

$$psN = 0.29 + 1598 * z_{\tau} \quad (9)$$

This way, the values for the yields ppN and psN vary according with the abundance reached in the ISM when stars forms⁶. For a CBM all stars form simultaneously, so we have taken for this metallicity the value Z_{τ} . The resulting yields are given in the two last rows of Table 3. For high metallicity regions, as the inner disc located at 2 kpc, Z_{τ} is higher than for a medium star formation region, as the Solar vicinity, and, therefore, ppN is lower, and $Z_N/Z_O = ppN/p$ will be also lower. This means that the exponential function shown in Fig. 3 increases until a smaller value. On the

⁵ Actually, in the multiphase models the maximum star formation moves toward later times for the outer regions compared with the early times in which the maximum occurs for the inner regions. Therefore, the Z_{τ} might be chosen taken into account this shift in the time scale respect of the zero time with which we have selected the values of Table 3.

⁶ This method is, in fact, an approximation: if ppN and psN depend on Z , it is necessary to perform a new integration and the final result is not equal to Eq. (3). We have checked that this approximation, easier to understand and to use, is enough good, giving a similar behaviour to the one obtained with the exact solution.

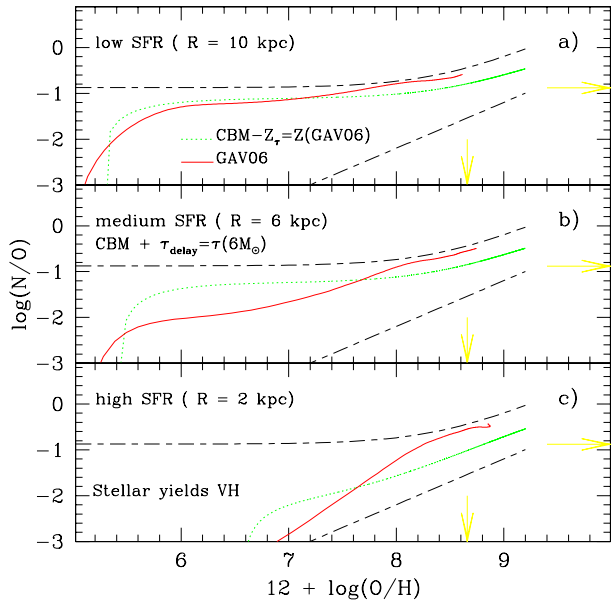


Figure 5. The relation N/O–O/H obtained using the stellar yields for LIM stars from VH, with the Galactic multiphase chemical evolution model from Gavilán et al. (2006), for three regions of the Galactic disc located at a) 10, b) 6 and c) 2 kpc galactocentric radius, solid (red) lines. Each line is compared with the CBM results (dotted green lines) computed assuming a delay $Z_\tau = Z(t = \tau(6M_\odot))$ taken from the corresponding region multiphase model, and using Eq.(8) and (9) as the dependent on metallicity yields psN and ppN . The short-long-dashed lines and the arrows have the same meaning than in Fig. 3.

Table 3. Values of oxygen abundances Z_τ reached when LIM stars of $6M_\odot$ died in the multiphase models VH from GAV06 and the corresponding values for psN and ppN

Radius (kpc)	Z_τ	OH_τ	ppN	psN
2	4.7E-5	6.60	2.01E-5	0.365
6	3.0E-6	5.40	1.66E-4	0.295
8	2.4E-6	5.30	1.99E-4	0.293
10	2.0E-6	5.24	2.23E-4	0.292
18	1.5E-6	5.10	2.83E-4	0.291

other hand, the value psN will be higher for the inner region than for the Solar Vicinity, and, consequently, the secondary behaviour due to LIM stars is stronger and more evident for the region at 2 kpc than for the one located at 6 or 10 kpc.

The same behaviour is apparent for the multiphase models. Thus, as it is evident in that figure, the metallicity dependent yields change the expected tracks in the figure N/O–O/H due to variations in the star formation rate, increasing the existing difference among them, specially if this star formation rate is strong enough. When it is very low, as it occurs in panel a), models give similar results than the corresponding ones to Fig.3. When these metallicity dependent yields are included in a model with strong star formation (panel c), the evolution changes appreciably compared with the equivalent track obtained with only one set of yields. This is reasonable: while Z is low, the model is similar to the one obtained with Q's matrices computed with yields for only one metallicity. When the

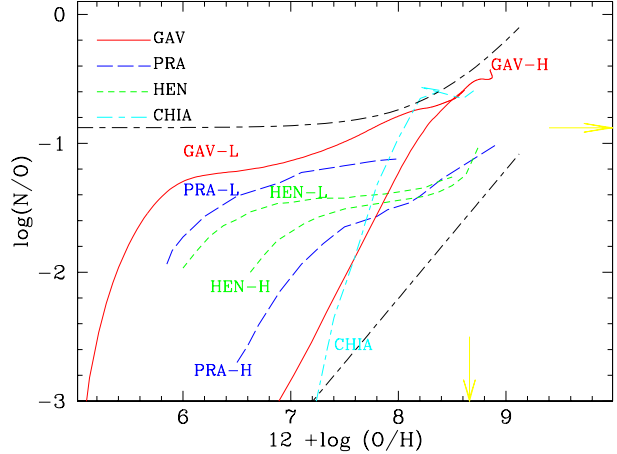


Figure 6. The evolution of the relative abundance $\log(N/O)$ with the oxygen evolution $12 + \log(O/H)$ for two multiphase chemical evolution models –GAV–, computed using the yields from van den Hoek & Groenewegen (1997) and Woosley & Weaver (1995) and the mean-lifetimes from Schaller et al. (1992), compared with that obtained in models from Henry et al. (2000); Prantzos (2003) –HEN and PRA, respectively, and Chiappini et al. (2003)–CHIA. The lines coding is given in the figure. Each model, except CHIA, is marked as L or H following the star formation rate is low or high. The short-long-dashed lines and the arrows have the same meaning than in previous figures.

oxygen abundance increases, the stellar production is computed using other set of yields. In particular, the yield of N increases but the contribution of NS is relatively higher than before and the NP, that gives the final flat level of N/O, is smaller. This way, the evolution of N/O in a strong star formation model behaves like more secondary and the exponential shape seems smoother.

3.4 Comparison with other works

From the previous section we have found that the track in the plane N/O–O/H result to be flat when the star formation is low and steep in the case of strong star formation. This effect is not new since, such as we have already mentioned, some other works, as Mouhcine & Contini (2002); Lanfranchi & Friaça (2003), have found a similar behaviour, a flattening of the track in the N/O–O/H plot, when the star formation efficiency decreases. As an example, we compare in Fig. 6 our results with those obtained by other authors. All of them were computed using the same set of yields from Woosley & Weaver (1995) for massive stars and from van den Hoek & Groenewegen (1997) for LIM stars. Our Galactic models for radial regions located at galactocentric radii $R = 2$ and 10 kpc are represented by the solid line. Since each radial region has its own total mass, gas infall rate, efficiencies, and volume, the star formation history results different for each one, slow and low in the outer region, and strong and early in the inner one. Correspondingly, they are marked as GAV-L and GAV-H, respectively. Other lines represent models from HEN, PRA and Chiappini et al. (2003), marked in the plot. The first two authors give two models with high (represented with an H) and low (represented with a L) star formation efficiency. Both authors obtained tracks rather flat in the plane N/O–O/H when the star formation is low, with a change of phase at $12 + \log(O/H) \sim 6 - 6.3$ while the strong star formation model show this feature at $12 + \log(O/H) \sim 7$. The Chiappini et al. (2003)'s model shows a steeper behaviour more according with our

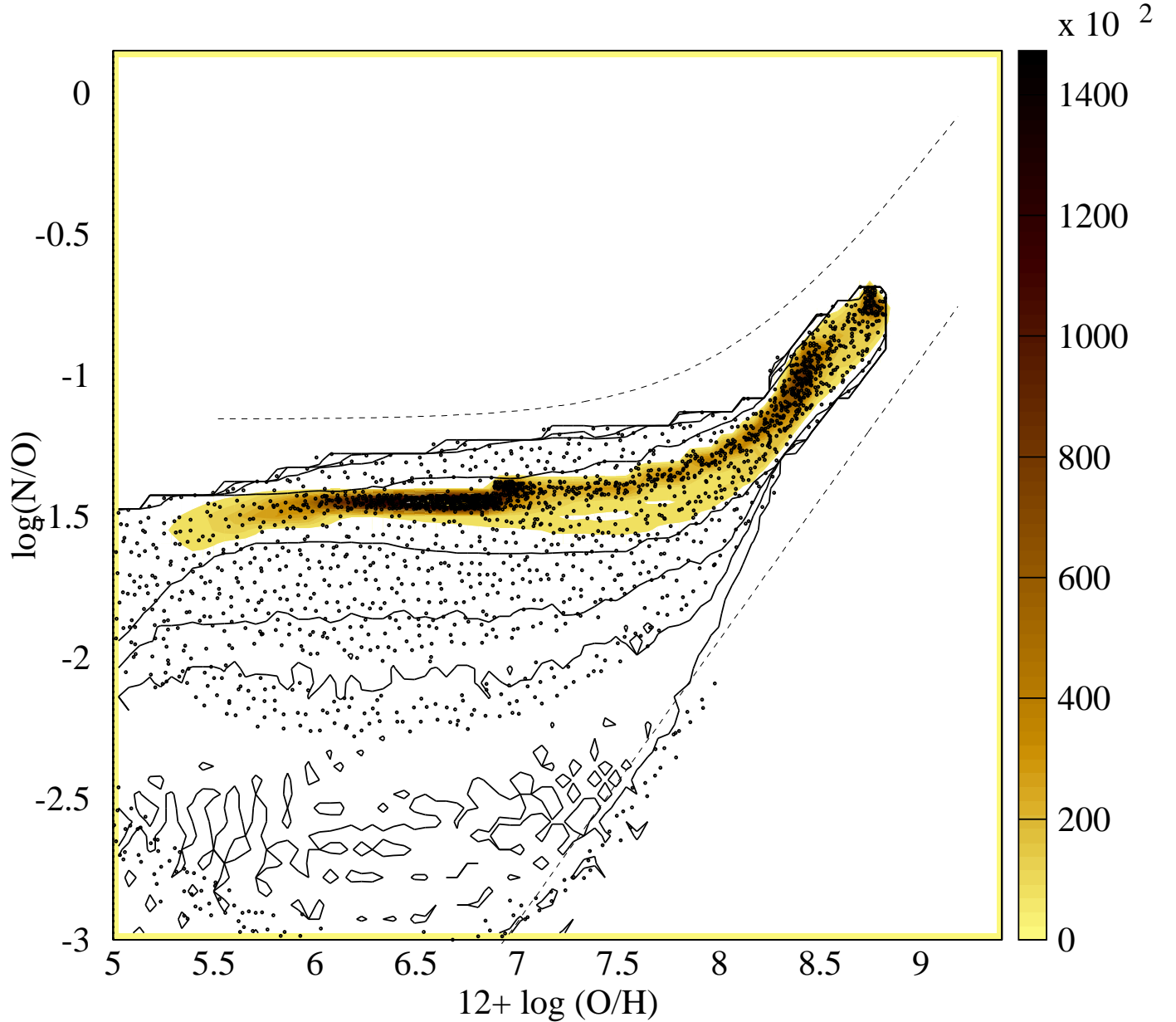


Figure 7. The relation between N/O and O/H for the simulated galaxies. The complete results for all modeled regions shown as small dots. Colored contours represent the isolines of number of points included within them (see relative scale to the right), while solid lines represent the regions with 0.3, 0.03, 0.012 and 0.003 %, respectively, of the total number of points. The data region is limited by the two dashed lines.

model for strong star formation, (probably due to their strong star formation in the halo).

Is is evident that our models behave similarly to others in what refers to the variation of N/O tracks with the usual input parameters of chemical evolution models. We claim that a flat behaviour for the evolution of N/O vs O/H is a usual characteristic of regions or galaxies where the star formation occurs quietly maintaining a low value for a long time. The presence of this flat behaviour in the N/O vs O/H plot is not only due to the used yields.

Since the effect of the star formation is important, it also appears using any other yield set with primary N ejected by LIM

stars. Obviously, the absolute values of the ratio N/O depend on the yields set used. GAV05 presented a set of LIM stars yields which are very similar to those calculated by Dray et al. (2003) from accurate stellar models – see Fig.5 from GAV06– but span a wider range in mass and metallicity as required in chemical evolution models. They were computed with a similar technique to that used by van den Hoek & Groenewegen (1997) but with updated inputs. The main difference between these two sets of yields resided in the contribution of primary (or secondary) component to the total nitrogen yield by LIM stars, which is larger in GAV05 by factors between 2 and 4 depending on metallicities, even though the total N

integrated yield is larger in van den Hoek & Groenewegen (1997) at all metallicities (see Fig.3 from GAV06). These yields were included and successfully calibrated in a GCE model in GAV05 and GAV06, reproducing the classical observational constraints (Star formation history, radial distributions of gas, etc.) and obtaining N abundances in agreement with the MWG stellar data. In particular, the flat behavior shown by the metal-poor star data of the Galactic halo results very well reproduced (see Fig.12 of GAV06).

4 THE GRID RESULTS: N/O VS O/H FOR SPIRAL AND IRREGULAR GALAXIES

The grid of chemical evolution models from Mollá & Díaz (2005)⁷ was parameterized by the initial mass radial distribution. For each one of our 44 theoretical galaxies, defined by this mass distribution, 10 different sets of efficiencies of molecular cloud formation and star formation were used, providing 10 evolutionary tracks. Thus, a total of 440 models were computed. For each one, a set of radial regions, variable according to the size of the theoretical galaxy, were modeled. Therefore, a large number of possible evolutionary tracks is finally available to compare with observations. The massive stars yields from WW and the above cited new yields for LIM stars from GAV05 have been used for calculating this grid of models. Even though that there are still some uncertainties in the AGB phase treatment and in the quantity of primary nitrogen that LIM stars may create, we consider that the set of stellar yields from GAV05 has been well calibrated and, therefore, that it is adequate to our purposes.

We ran models that represent the evolution of different regions of galaxies, assuming that there is also star formation in the halo (with a constant efficiency for all models), and that infall rates, initial masses of gas and efficiencies to form stars are all different from a modeled galaxy to the following one. All these factors multiply their effects, changing the resulting star formation history. Thus, the final results show very different evolutions of the N/O vs O/H as we will show in the following figures.

In Fig. 7 we show the results for the relative abundance $\log(N/O)$ vs the oxygen abundance, $12 + \log(O/H)$ obtained with an updated grid of models, computed with the same inputs and hypotheses than Mollá & Díaz (2005) but using as stellar mean-lifetimes those computed from Schaller et al. (1992), instead those ones from Burkert & Hensler (1987) used in our previous version. There we show the whole set of results,⁸ for all calculated times⁹ and models, as small dots. Over them we have plot some contours in yellow levels, defined by the scale located at the right. Furthermore, we draw some other contours as solid lines for regions with 0.3, 0.03, 0.012 and 0.003 %, respectively, of the total number of points.

It is evident that the generic trend obtained with our models using the new yield set looks very similar to that shown by the data which lie in the region defined by the dashed lines. The predicted dispersion is also large, as shown by the observations.

In Fig. 8 we only represent the present time results, as full

⁷ See this work for details about the chemical evolution models, available in <http://vizier.u-strasbg.fr/viz-bin/VizieR?-source=J/MNRAS/358/521>

⁸ These updated results are available in electronic format in http://wwwae.ciemat.es/~mercedes/grid_chemev.html

⁹ The time step used for writing results is 0.1 Gyr. Obviously if we plot results with a smaller time step, the graph will result more densely populated

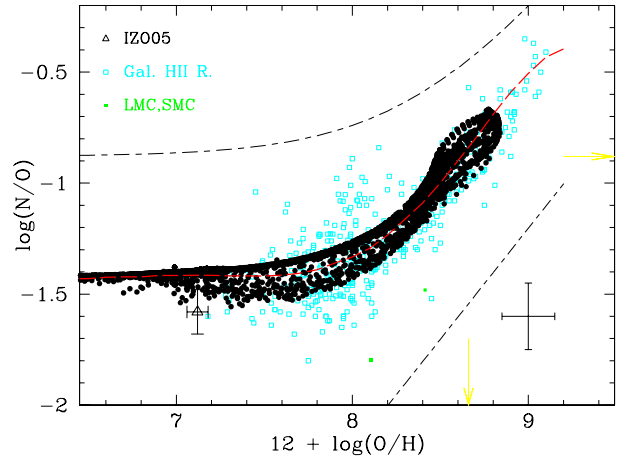


Figure 8. The relative abundance $\log(N/O)$ vs the oxygen abundance $12 + \log(O/H)$ for the present time as full (black) dots compared with the data corresponding to Galactic and extragalactic HII regions, represented as ion (cyan) squares. The long-dashed (red) line is the least squares fitting function. The large open triangle around $12 + \log(O/H) \sim 7.1$ is the value found by Izotov et al. (2005) for the lowest-metallicity star-forming galaxy known. The short-long-dashed lines and the arrows have the same meaning than in Fig. 3.

points, that we compared with the Galactic and extragalactic HII regions data, as open squares, taken from references given in Table 1. Our models may be fitted by a least-squares polynomial function, shown by a long-dashed line in the same plot:

$$\log(N/O) = -1149.31 + 1115.23x - 438.87x^2 + 90.05x^3 - 10.20x^4 + 0.61x^5 - 0.015x^6$$

where $x = 12 + \log(O/H)$.

It is evident that our models reproduce adequately the trend of present day data and, even, a certain dispersion. There are two zones where data fall out of the models region. The first one corresponds to the high metallicity HII ($Z > Z_\odot$) regions, where it is difficult to estimate directly elemental abundances. In fact, recent estimations for some of this kind of regions seem to produce lower oxygen abundances than the old ones, estimated through other empirical methods (Castellanos et al., 2002; Pilyugin, 2004). Therefore, it is probable that those points must be corrected. The second region correspond to oxygen abundances around $12 + \log(O/H) = 8$, just when the parameter R_{23} , usually used to estimate O/H in the low metallicity regions, is bi-valuated, thus increasing the data errors above the usual error bar (shown in the plot). On other hand, it is well known that some nearby star-forming galaxies show evidence of galactic winds and there are a large number of works (Marcolini et al., 2004; Hensler et al., 2004; Recchi et al., 2006; Recchi & Hensler, 2006; Romano et al., 2006) including this possibility in their evolution models. We cannot discard the existence of outflows in the galaxies whose data our models do not reproduce, and, maybe this is the solution of this disagreement. However, in general, these winds are important only in young ($< 10^7$ yr) starbursts that form many massive stars in a metal rich environment ($Z > Z_\odot$) (Veilleux et al., 2005). Recent RX observations (Rasmussen et al., 2004; Ott et al., 2005; Grimes et al., 2005) show evidences of these winds in dwarf galaxies, but only for those suffering a starburst, which means $SFR > 5M_\odot \text{yr}^{-1}$. This high star formation rate is not always present in dwarf galaxies. On the other hand, the dwarf irregular galaxies with rotation velocity higher than

30 km.s⁻¹ seem able to retain their gas-rich disks (Garnett, 2002; Dekel & Woo, 2003). Thus, the discussion of this subject requires a study for individual galaxies which fall out of the scope of this work and which we hope treat in the next future. In any case the least squares fitting function, also represented in the figure, has a behaviour in agreement with the generic trend of data, even at the high-abundance end.

In order to see the effects of the galaxy total mass and/or the variations of the star formation efficiencies on the computed abundances, we show in Fig. 9 the evolutionary tracks of N/O abundances for two limiting models: 1) that corresponding to the most massive galaxy with the highest molecular cloud and star formation efficiencies –model M, solid lines– and 2) that corresponding to the less massive galaxy and with the smallest efficiencies –model L, dotted lines–. Each line represent various radial regions in a same time step, given in the plot in Gyr. We would like to stress that these lines are not evolutionary tracks in time. To obtain that, it is necessary to join the points corresponding to a given radial region of a galaxy at different time steps as we have done with the short-dashed line. It is clear from this plot that the exact mode in which the star formation takes places determines the evolution of the N/O ratio. In the first type of galaxy, there is an intense star formation episode, occurring early in time and declining afterward, simulating an early morphological type bright galaxy. The second example shows a low and continuous star formation rate producing an object similar to a dwarf galaxy. In the first case N/O evolves very quickly showing a secondary trend, beginning from $\log(N/O) \sim -2.5$ dex when the oxygen abundance is already $12 + \log(O/H) \sim 7$ dex, while in the second N/O keeps a very constant value of $\log(N/O) \sim -1.4$ dex along the whole evolution, with oxygen abundances $12 + \log(O/H) \leq 7$. These two models define a region similar to the one predicted by Vila Costas & Edmunds (1993, see their Fig.A1), but for the opposite reason: the less evolved models have higher N/O ratios than the ones with strong star formation rates and smaller time delays.

Thus, the abundances shown by some metal-poor dwarf galaxies, can be reproduced by models with a continuous star formation rate with low efficiencies. This is so, even taking into account the lifetimes of the LIM. In fact a delay in the ejection of N does not necessarily imply a low value of N/O. On the one hand because the time required to reach the N/O value shown by BCD ($\log N/O \simeq -1.5$) might be as short as $\sim 300 - 400$ Myr, since intermediate mass stars of $4 - 8 M_{\odot}$ (which contribute to the primary N), have mean-lifetimes in the range $50 \leq \tau \leq 200$ Myr. On the other hand, and more important, because low oxygen abundances does not imply necessarily a short evolutionary time since with a low star formation it is possible to maintain a low value of O/H for a long time.

These results are only partially due to the dependence with metallicity of the yields we use. The integrated ratio of primary to total N yields $^{14}\text{N}_p/^{14}\text{N}$ (see Fig.3 from Gavilán et al., 2006) has a value ~ 0.20 for Z_{\odot} (slightly smaller than the one estimated, $\sim 1/3$, by Alloin et al., 1979, as necessary to reproduce the data) and it increases up to 0.6 for low metallicities. This contribution of primary N, larger for low metallicity stars than for high metallicity ones, is important since it allows to us to obtain tracks in the plane N/O vs O/H flatter than the ones predicted with a constant contribution of the primary N. We must to do clear, however, that if we eliminate the metallicity dependence from the yields, we still obtain different tracks for regions with different star formation histories, as we have shown in previous sections. Thus, the selection of the set of yields is not essential to obtain these differences among tracks, although the shown effect increases when metallicity-dependent yields are

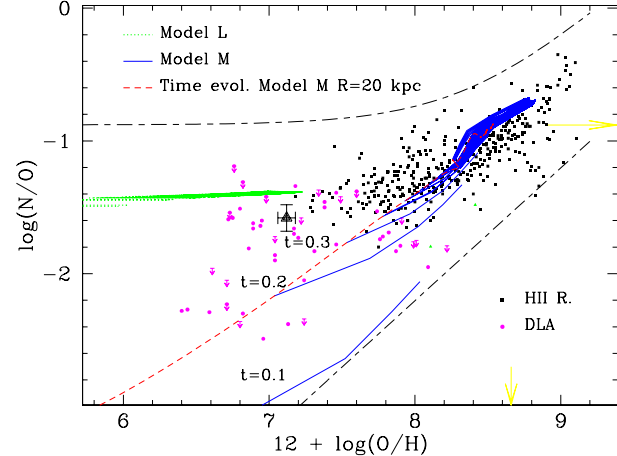


Figure 9. The relation between N/O and O/H for the most evolved and most massive galaxy, model M, solid (blue) lines, and for the lowest mass and less evolved galaxy, model L, dotted (green) lines, while the short-dashed (red) line indicates the time evolution of a region at 20 kpc of galactocentric distance of model M. The small full squares are the HII regions data, while the full (magenta) dots are the DLA objects data. The large triangle around $12 + \log(O/H) \sim 7.1$ is the value found by Izotov et al. (2005) for the lowest-metallicity star-forming galaxy known. The short-long-dashed lines and the (yellow) arrows have the same meaning than in Fig. 3.

included in the models. Furthermore, the absolute level of observations and the fine tuning of the observed shape in the plane N/O-O/H for the present time data is only reproduced if the stellar yields, in turn, give the right level of primary nitrogen and have the adequate dependence on metallicity. The chemical evolution models must also be well calibrated in order to predict star formation histories able to produce abundances in agreement with data. Therefore, the adequate selection of metallicity dependent LIM star yields, as those from GAV05, joined to the use of accurate chemical evolution models, as those from Mollá & Díaz (2005), allows to obtain abundances for N and O which reproduce the complete set of data in the plane N/O vs O/H.

Finally, in order to explore the time evolution of the modeled abundances, we show in Fig. 10 the results for four different time steps: $t = 0.1$, $t = 0.17$, $t = 0.30$, and $t = 13.2$ Gyr. These epochs would correspond to redshifts $z \sim 3.8, 3.7, 3.5$, and 0, respectively, for a cosmology with $H_0 = 71$, $\Omega_M = 0.30$, $\Omega_{\Lambda} = 0.70$, if the formation of these spiral and irregular galaxies occurred at a redshift $z \sim 4$. A large gap appears between the results for each one of our time steps. In particular, our models predict a feature similar to the so-called *second plateau* that Centurión et al. (2003) claim to exist at a metallicity around $12 + \log(O/H) \sim 7$, which appears at a level of $\log(N/O) \sim -2.3$ for $12 + \log(O/H) \sim 6.5 - 7$, while most points appear at a higher level of N/O (≥ -1.8) for a similarly low O/H abundance. In fact, no gap is apparent between models at 1.1 and 13.2 Gyr, thus making it difficult to discriminate objects at a redshift up to $z < 2.5$ from those at redshift $z=0$ in the N/O-O/H plane, as it is actually the case. The abundances predicted for galaxies at redshift $z \geq 3$ are far enough from the rest of the points in the plot so as to disentangle them from a given data sample.

Thus, the abundance data from DLA objects are easily reproduced by models of massive galaxies with strong star formation in the early stages of their evolution. This evolution is so rapid in those galaxies that 300 Myr after the beginning of the formation of stars the value of $\log(N/O)$ increases from -2.5 to -1.6 with oxygen abun-

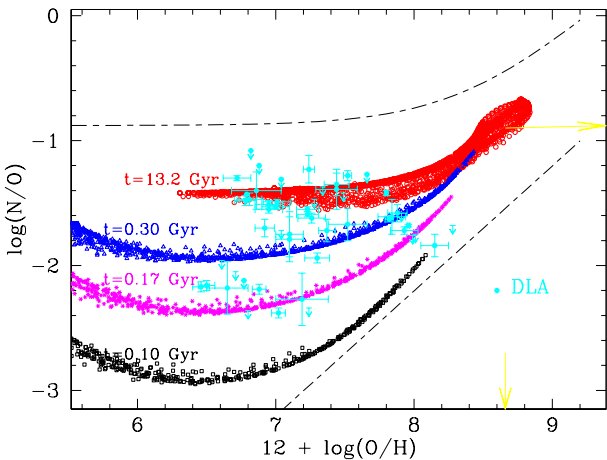


Figure 10. The relation N/O – O/H for different evolutionary times as marked in the figure. Full (magenta) dots correspond to DLA objects.

dances $12 + \log(\text{O/H}) = 7 - 8.5$. Therefore, it should be possible to find objects in this zone of the N/O vs O/H plot, although, given the shortness of this phase, the number of these objects would be small. We note that a level of $\log(\text{N/O}) \sim -1.6$ dex is easily reached in such a short time, in galactic evolutionary terms, as $t \sim 300 \text{ Myr}$, even with a primary contribution proceeding from LIM stars.

5 CONCLUSIONS

The evolutionary track followed by a given region or galaxy in the N/O vs O/H plane depends strongly on the star formation history of the region. Strong bursting star formation histories would produce high oxygen abundances soon and, hence, an early secondary behaviour, thus reproducing most of the spiral H_{II} region observations. On the contrary, a low and continuous star formation rate keeps the oxygen abundance low for a long time; thus a large quantity of primary N may be ejected reproducing the flat slope shown by dwarf galaxy data.

The resulting dispersion of our realizations, similar to the one observed, appears as a consequence of the different star formation histories in each modeled region and in each galaxy. These are obtained by combining various star and molecular cloud formation efficiencies and collapse time scales.

The stellar yields for LIM also play a role: if they have the adequate contribution of primary N depending on metallicity, it is easy to reproduce adequately the generic trend of the observational points in the N/O vs O/H plane, in particular a flat slope for low metallicity regions and, simultaneously, lower values of N/O at similar oxygen abundances for regions or galaxies where the star formation is strong and occurred early in the evolution.

The combination of the new yield set from Gavilán et al. (2005) and the self-consistent chemical evolution models by Mollá & Díaz (2005) are able to reproduce the data corresponding to H_{II} regions in different galaxies and Galactic stars of different ages. This arises naturally just by assuming different input parameters (mostly star formation efficiencies and infall rates) for the different galaxies and regions in the same generic model, without the need to appeal to *ad hoc* models to reproduce each kind of object.

They may also reproduce the existing data on galaxies at $0 \leq z \leq 4$, and predict the existence of a second plateau, found in the N/O vs O/H relationship for $\log(\text{N/O}) \sim -2.5$ and galaxies

with $z \geq 3$. Our models predict that objects at redshifts $z \leq 2.5$ can not be discriminated from $z = 0$ objects in the log(N/O) vs log(O/H) plane; however, for $z \geq 3$ objects, this discrimination is possible. This characteristic is a consequence of the rapid passage of model results by this zone of the plane, when the time evolution is considered, since 300 Myr after the beginning of the formation of stars, the value $\log(\text{N/O})$ increases from -2.5 to -1.6 with oxygen abundances $12 + \log(\text{O/H}) = 7 - 8.5$

ACKNOWLEDGMENTS

This work has been partially supported by the Spanish PNAYA project AYA2004-8260-C03. We acknowledge their comments to R.B.C Henry and L. Pilyugin who have kindly revised part of this manuscript. We thank an anonymous referee for the useful comments and suggestions that have improved this paper.

REFERENCES

- Alloin D., Collin-Souffrin S., Joly M., Vigroux L., 1979, A&A, 78, 200
- Barbuy B., 1983, A&A, 123, 1
- Burkert A., Hensler G., 1987, Lecture Notes in Physics, Berlin Springer Verlag, 287, 159
- Cairós L. M., García-Lorenzo B., Caon N., Vílchez J. M., Pápareros P., Noeske K., 2003, Ap&SS, 284, 611
- Carbon D. F., Barbuy B., Kraft R. P., Friel E. D., Suntzeff N. B., 1987, PASP, 99, 335
- Carigi L., Peimbert M., Esteban C., García-Rojas J., 2005, ApJ, 623, 213
- Castellanos M., Díaz A. I., Terlevich E., 2002, MNRAS, 329, 315
- Centurión M., Molaro P., Vladilo G., Péroux C., Levshakov S. A., D'Odorico V., 2003, A&A, 403, 55
- Chiappini C., Hirschi R., Meynet G., Ekström S., Maeder A., Matteucci F., 2006, A&A, 449, L27
- Chiappini C., Matteucci F., Ballero S. K., 2005, A&A, 437, 429
- Chiappini C., Matteucci F., Meynet G., 2003, A&A, 410, 257
- Clegg R. E. S., Tomkin J., Lambert D. L., 1981, ApJ, 250, 262
- Contini T., Treyer M. A., Sullivan M., Ellis R. S., 2002, MNRAS, 330, 75
- Daflon S., Cunha K., 2004, ApJ, 617, 1115
- Dekel A., Woo J., 2003, MNRAS, 344, 1131
- Dray L. M., Tout C. A., Karakas A. I., Lattanzio J. C., 2003, MNRAS, 338, 973
- Edmunds M. G., Pagel B. E. J., 1978, MNRAS, 185, 77P
- Esteban C., Peimbert M., Torres-Peimbert S., 1999, A&A, 342, L37
- Esteban C., Peimbert M., Torres-Peimbert S., García-Rojas J., 1999, Revista Mexicana de Astronomía y Astrofísica, 35, 65
- Esteban C., Peimbert M., Torres-Peimbert S., García-Rojas J., Rodríguez M., 1999, ApJs, 120, 113
- Ferrini F., Matteucci F., Pardi C., Penco U., 1992, ApJ, 387, 138
- Ferrini F., Mollá M., Pardi M. C., Díaz A. I., 1994, ApJ, 427, 745
- Fich M., Silkey M., 1991, ApJ, 366, 107
- Garnett D. R., 2002, ApJ, 581, 1019
- Garnett D. R., Shields G. A., Peimbert M., Torres-Peimbert S., Skillman E. D., Dufour R. J., Terlevich E., Terlevich R. J., 1999, ApJ, 513, 168

Garnett D. R., Skillman E. D., Dufour R. J., Peimbert M., Torres-Peimbert S., Terlevich R., Terlevich E., Shields G. A., 1995, *ApJ*, 443, 64

Gavilán M., Buell J. F., Mollá M., 2005, *A&A*, 432, 861

Gavilán M., Mollá M., Buell J. F., 2006, *A&A*, 450, 509

Gratton R. G., Sneden C., Carretta E., Bragaglia A., 2000, *A&A*, 354, 169

Grimes J. P., Heckman T., Strickland D., Ptak A., 2005, *ApJ*, 628, 187

Gummersbach C. A., Kaufer A., Schaefer D. R., Szeifert T., Wolf B., 1998, *A&A*, 338, 881

Henry R. B. C., Edmunds M. G., Köppen J., 2000, *ApJ*, 541, 660

Hensler G., Theis C., Gallagher J. S. I., 2004, *A&A*, 426, 25

Hirschi R., 2005, in Hill V., François P., Primas F., eds, IAU Symposium PopII 1/2 stars: very high 14N and low 16O yields. pp 331–332

Israelian G., Ecuvillon A., Rebolo R., García-López R., Bonifacio P., Molaro P., 2004, *A&A*, 421, 649

Izotov Y. I., Thuan T. X., 1999, *ApJ*, 511, 639

Izotov Y. I., Thuan T. X., Guseva N. G., 2005, *ApJ*, 632, 210

Laird J. B., 1985, *ApJ*, 289, 556

Lanfranchi G. A., Friça A. C. S., 2003, *MNRAS*, 343, 481

Larsen T. I., Sommer-Larsen J., Pagel B. E. J., 2001, *MNRAS*, 323, 555

Legrand F., 2000, *A&A*, 354, 504

Marcolini A., Brighenti F., D'Ercole A., 2004, *MNRAS*, 352, 363

Marigo P., Bressan A., Chiosi C., 1998, *A&A*, 331, 564

McCall M. L., Rybski P. M., Shields G. A., 1985, *ApJs*, 57, 1

Meynet G., Maeder A., 2002, *A&A*, 390, 561

Mollá M., Díaz A. I., 2005, *MNRAS*, 358, 521

Mollá M., Ferrini F., Díaz A. I., 1996, *ApJ*, 466, 668

Mouhcine M., Contini T., 2002, *A&A*, 389, 106

Nava A., Henry R. B. C., Prochaska J. X., 2005, in Revista Mexicana de Astronomía y Astrofísica Conference Series The Distribution of Metal Poor Galaxies in the N/O Plateau. pp 117–117

Ott J., Walter F., Brinks E., 2005, *MNRAS*, 358, 1453

Pagel B. E. J., Edmunds M. G., Blackwell D. E., Chun M. S., Smith G., 1979, *MNRAS*, 189, 95

Peimbert M., 1979, in IAU Symp. 84: The Large-Scale Characteristics of the Galaxy Chemical evolution of the galactic interstellar medium - Abundance gradients. pp 307–315

Pettini M., Ellison S. L., Bergeron J., Petitjean P., 2002, *A&A*, 391, 21

Pilyugin 2004, *A&A*, 423, 427

Pilyugin L. S., Thuan T. X., Vilchez J. M., 2003, *A&A*, 397, 487

Portinari L., Chiosi C., Bressan A., 1998, *A&A*, 334, 505

Prantzos N., 2003, in Astronomical Society of the Pacific Conference Series Evolution of CNO Abundances in the Universe. pp 361–+

Prochaska J. X., Henry R. B. C., O'Meara J. M., Tytler D., Wolfe A. M., Kirkman D., Lubin D., Suzuki N., 2002, *PASP*, 114, 933

Rasmussen J., Stevens I. R., Ponman T. J., 2004, *MNRAS*, 354, 259

Recchi S., Hensler G., 2006, *A&A*, 445, L39

Recchi S., Hensler G., Angeretti L., Matteucci F., 2006, *A&A*, 445, 875

Renzini A., Voli M., 1981, *A&A*, 94, 175

Romano D., Tosi M., Matteucci F., 2006, *MNRAS*, 365, 759

Schaller G., Schaerer D., Meynet G., Maeder A., 1992, *A&AS*, 96, 269

Serrano A., 1986, *PASP*, 98, 1066

Shaver P. A., McGee R. X., Newton L. M., Danks A. C., Pottasch S. R., 1983, *MNRAS*, 204, 53

Smartt S. J., Venn K. A., Dufton P. L., Lennon D. J., Rolleston W. R. J., Keenan F. P., 2001, *A&A*, 367, 86

Spite M., Cayrel R., Plez B., Hill V., Spite F., Depagne E., François P., Bonifacio P., Barbuy B., Beers T., Andersen J., Molaro P., Nordström B., Primas F., 2005, *A&A*, 430, 655

Thuan T. X., Izotov Y. I., 2005, *ApJ*, 627, 739

Thuan T. X., Izotov Y. I., Lipovetsky V. A., 1995, *ApJ*, 445, 108

Tinsley B. M., 1980, *Fundamentals of Cosmic Physics*, 5, 287

Tolstoy E., 2003, *Ap&SS*, 284, 579

Tomkin J., Lambert D. L., 1984, *ApJ*, 279, 220

Tsamis Y. G., Barlow M. J., Liu X.-W., Danziger I. J., Storey P. J., 2003, *MNRAS*, 338, 687

van den Hoek L. B., Groenewegen M. A. T., 1997, *A&As*, 123, 305

van Zee L., Barton E. J., Skillman E. D., 2004, *AJ*, 128, 2797

van Zee L., Haynes M. P., 2006, *ApJ*, 636, 214

van Zee L., Salzer J. J., Haynes M. P., O'Donoghue A. A., Balonek T. J., 1998, *AJ*, 116, 2805

van Zee L., Skillman E. D., Haynes M. P., 2006, *ApJ*, 637, 269

Veilleux S., Cecil G., Bland-Hawthorn J., 2005, *ARA&A*, 43, 769

Vila Costas M. B., Edmunds M. G., 1993, *MNRAS*, 265, 199

Vilchez J. M., Esteban C., 1996, *MNRAS*, 280, 720

Woosley S. E., Weaver T. A., 1986, *Lecture Notes in Physics*, Berlin Springer Verlag, 255, 91

Woosley S. E., Weaver T. A., 1995, *ApJs*, 101, 181